Numerical Models of Water Wave with Parabolic and Hyperbolic Forms

Lee, Jong-Kyu* / Lee, Chang-Hae**

ABSTRACT/The numerical models of the parabolic equation, applicable only to the progressive wave, and hyperbolic equation, which may consider even the reflected wave, were developed and applied to the area of the submerged circular shoal and then results obtained from both models were compared with experimental measurements and each other. The hyperbolic model was further applied to both the detached breakwater and the breakwater with a gap. The numerical results were plotted and compared with the existing data. Numerical solutions were obtained with the finite difference method.

1. Introduction

Waves travelling in the sea do not experience the deformation of their characteristics before the water depth becomes nearly half of the wave length. As these waves are approaching toward nearshore, waves go through some changes of wave characteristics due to shoaling, refraction, diffraction and reflection. Previous investigations on wave transformation are mostly based on the measurements in the field and physical modelling which require a great deal of effort and time. With the advent of large memory and high speed computers, it became popular to analyze the wave transformation numerically in economic aspect.

Berkhoff(1972) first drived an elliptic type equation, which is called mild-slope equation and well describes the characteristics of wave transformation influenced by shoaling, refraction, diffraction and reflection, by integrating three dimensional velocity potential equation over the depth and incorperating boundary conditions at free-surface and bottom under the assumption that bottom slope is mild and terms higer than the second order can be neglected. An elliptic equation takes the form of a boundary value problem and reqires the solution of a large mumber of simultaneous equations. According to Booij(1981), the

* Prof., Dept., of Civil Eng., Hanyang Univ.

** Graduate Student, Dept., of Civil Eng., Hanyang Univ.

increased computation time and difficulty involved in the solution of an elliptic equation make it much less useful than the solution of a hyperbolic or parabolic equation.

Substituting wave's time-harmonic variable, the mild-slope equation can be represented in term of wave amplitude. This parabolic approximation is done by Radder(1979), Kirby(1983), Liu(1983), and Liu and Tsay(1984). Lee and Lee(1990) applied the parabolic type equation based on Liu and Tsay's mathematical model(1984) to the rigion where the circular shoal is existing. The use of the parabolic model may be limited if wide-angled diffraction occurs, because the energy transfer in one of the co-ordinates is ignored in the mathematical formulation(Yoo et al., 1988). Therefore the parabolic model is not capable of diffraction analysis of the back side of breakwater. Moreover the parabolic approximation is not adequate for the case of the wave field with a strongly reflecting structure.

Copeland(1985) has presented the mild-slope equation in the form of a pair of first-order equations, which constitute a hyperbolic system, without the loss of the refleced wave. The hyperbolic model can consider the effect of refraction, diffraction and reflection with accuracy of the mild-slope equation, and can also be formulated as an initial value problem.

The parabolic and the hyperbolic numerical models developed here were applied to the calculation of wave height distribution in the region of the submerged circular shoal. Only the hyperbolic model was applied to the wave field around the breakwater.

The first purpose of this study is to develope the numerical models of two types of equations above mentioned and to compare the results obtained from the application of each model to the circular shoal. The second one is on the applicability of the hyperbolic model in the vicinity of breakwater with the various bottom slope, incident angle and reflectivity.

2. Governing Equation

The theory of the mild-slope equation is restricted to irrotational linear simple harmonic waves, and loss of energy due to friction or breaking is not taken into account. The two-dimensional mild-slope equation which is applicable to waves in the range from shallow water to deep water has been derived by means of a small parameter development and an integration over the water depth(Berkhoff, 1972):

$$\nabla \cdot (CC_g \nabla \phi) + \omega^2 \frac{C_g}{C} \phi = 0 \tag{1}$$

where $\phi(x, y)$ is the velocity potential obtainted by factoring out the vertical component and the harmonic time dependence

C is the phase velocity $=\omega/k$

C_g is the group velocity of the wave $=d\omega/dk$

ω is the angular frequency $(=kC)$

k is the wave number $(=2\pi/\text{wave length})$, and

x, y are the principal direction of wave propagation and the lateral direction, respectively.

For the purpose of representing the mild-slope equation by the surface elevation η, the relation between η and ϕ is taken from the linearized dynamic free surface boundary condition:

$$\eta(x,y,t) = (i\omega/g)\,\phi(x,y)\,\exp(-i\omega t) \tag{2}$$

Substitution of Eq. (2) into Eq. (1) reduces to:

$$\nabla\cdot(CC_g\,\nabla\eta) + \omega^2\frac{C_g}{C}\,\eta = 0 \tag{3}$$

In order to drive the parabolic equation, it was assumed that only the progressive waves propagate on the slowly varying depth and the amplitude envelope varies more slowly in the direction of wave propagation than in the lateral direction.

In addition, when we take the surface elevation η at t=0, η can also be expressed by:

$$\eta(x,y) = A(x,y)\mathrm{Exp}\left(i\int^{x}\bar{k}\,dx\right) \tag{4}$$

where k, which is a function of x, is the wave numer of mean depth h which is averaged with depth through the y direction.

From the substitution of Eq. (4) into Eq. (3), we can obtain the partial differential equation in parabolic form as follows:

$$2ik\frac{\partial A}{\partial x} + \frac{1}{CC_g}\frac{\partial}{\partial y}\left(CCg\frac{\partial A}{\partial y}\right) + \left[\,i\frac{1}{CC_g}\left(\frac{\partial(kCC_g)}{\partial x}\right) + (k^2-\bar{k}^2)\right]A = 0 \tag{5}$$

where Eq. (5) was derived with omitting the terms higher than the second order.

Next, differentiating Eq. (2) twice with respect to time, we get:

$$\frac{\partial^2\eta}{\partial t^2} = -\,\omega^2\,\eta \tag{6}$$

Substitution of Eq. (6) into Eq. (3),

$$\nabla\cdot(CC_g\,\nabla\eta) - \frac{C_g}{C}\frac{\partial^2\eta}{\partial t^2} = 0 \tag{7}$$

Eq. (7) has hyperbolic form. This equation can be expressed as a pair of first-order equations, according to Copeland(1985), which has the same form as those obtained by Ito and Tanimoto(1972):

$$\nabla Q + \frac{C_g}{C}\frac{\partial\eta}{\partial t} = 0 \tag{8}$$

and

$$\frac{\partial Q}{\partial t} + CC_g \nabla \cdot \eta = 0 \tag{9}$$

where Q is a vertically integrated function of particle velocity.

3. Numerical Models

3.1. Parabolic Model

Numerical solution of the parabolic equation is a initial value problem without the downwave boundary condition, so a forward marching system may be used to solve three diagonal matrix along the direction of wave propagation. The finite difference numerical scheme is constructed by taking forward difference scheme as a time-like variable in the x(wave propagation) direction and central difference scheme in the y direction. The Crank-Nicholson implicit method is used for this scheme. Then the finite difference form of Eq. (5) can be arranged as follows:

$$C_1 \cdot A_{j-1}^{i+1} + C_2 \cdot A_j^{i+1} + C_3 \cdot A_{j+1}^{i+1} = C_4 \tag{10}$$

where,

$$C_1 = -B_2 + B_3 , \qquad C_2 = B_1 - 2B_2 + B_3 , \qquad C_3 = B_2 + B_3$$

$$C_4 = (B_2 - B_3)\, A_{j-1}^{i} + (B_1 + 2B_2 - B_4)\, A_j^{i} - (B_2 - B_3)\, A_{j+1}^{i}$$

$$B_1 = \frac{i}{\Delta x}\,(\bar{k}^{i+1} + \bar{k}^{i})$$

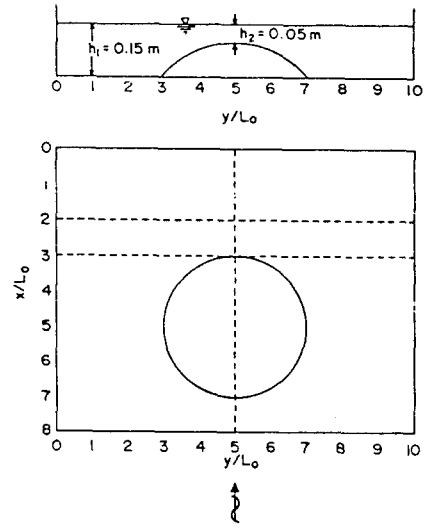

Fig. 1. Configuration for experiment of I to and Tanimoto.

$$B_2 = \frac{B_3}{4} \frac{\{(CC_g)_{j+1}^{i+1} - (CC_g)_{j-1}^{i+1} + (CC_g)_{j+1}^{i} - (CC_g)_{j-1}^{i}\}}{\{(CC_g)_j^{i+1} - (CC_g)_j^{i}\}}$$

$$B_3 = \frac{1}{2\,\Delta y^2}$$

$$B_4 = \frac{1}{2}\left[\frac{2\,i}{(CC_g)_j^{i+1} - (CC_g)_j^{i}}\{(\bar{k}CC_g)_j^{i+1} - (\bar{k}CC_g)_j^{i}\} + \left(\frac{k_j^{i+1} + k_j^{i}}{2}\right)^2 - \left(\frac{\bar{k}^{i+1} + \bar{k}^{i}}{2}\right)^2\right]$$

As the boundary condition to have the solution of Eq. (10), the no-flux condition is used along the y direction, thus:

$$\frac{\partial A}{\partial y} = 0 \qquad \text{at} \quad y \to \pm\infty \tag{11}$$

and the finite-difference form is:

$$A_{j+1}^{i+1} = A_{j-1}^{i+1} \qquad \text{at} \quad y \to \pm\infty \tag{12}$$

As the initial conditions, the experimental data of Ito and Tanimoto(1972) was taken and the details are presented in Fig. 1:

$h_1 = 0.15\ m,\ h_2 = 0.05\ m,\ H_0 = 0.0064\ m$

$T = 0.510812\ sec,\ L_0 = 0.4\ m,\ \Delta x = 0.05\ m,\ \Delta y = 0.05\ m$

where L_0 is the incident wave length.

3. 2. Hyperbolic model

The explicit finite differnce method is constructed, based on taking forward difference in the x, y and t direction for Q and the t direction for η, and backward difference in the x and y direction for η (Lee, 1990). The finite difference forms of Eq. (8) and Eq. (9) reduce to:

$$\eta_{i,j}^{t+\Delta t/2} = \eta_{i,j}^{t-\Delta t/2} - \left(\frac{C}{C_g}\right)_{i,j}[Qx_{i+1,j}^{t} - Qx_{i,j}^{t}]\frac{\Delta t}{\Delta x} - \left(\frac{C}{C_g}\right)_{i,j}[Qy_{i+1,j}^{t} - Qy_{i,j}^{t}]\frac{\Delta t}{\Delta y} \tag{13}$$

$$Qx_{i,j}^{t+\Delta t} = Qx_{i,j}^{t} - (CC_g)_{i,j}\,[\eta_{i,j}^{t+\Delta t/2} - \eta_{i-1,j}^{t+\Delta t/2}]\,\frac{\Delta t}{\Delta x} \tag{14}$$

$$Qy_{i,j}^{t+\Delta t} = Qy_{i,j}^{t} - (CC_g)_{i,j}\,[\eta_{i,j}^{t+\Delta t/2} - \eta_{i,j-1}^{t+\Delta t/2}]\,\frac{\Delta t}{\Delta y} \tag{15}$$

where the subscript i and j indicate increments in the x and y direction, respectively. Superscript t indicates evaluation at time t. The variables are located in the rectangular grid shown in Fig. 2. Note that the locations of the integrated component velocities Qx and Qy are offset from the locations of the surface elevation η by $\Delta x/2$ and $\Delta y/2$, respectively. It is apparent from the finite-difference equations that the values of Qx and

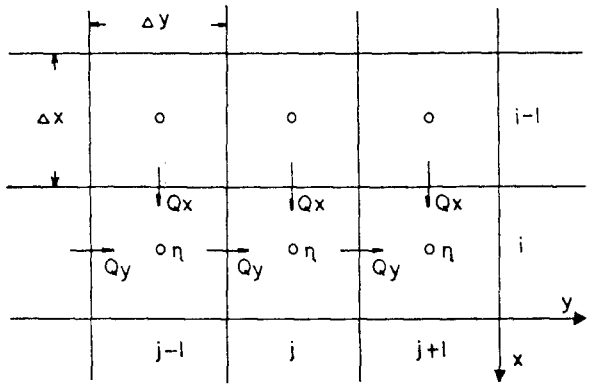

Fig. 2. The finite-difference mesh for hyperbolic model.

Qy are calculated at a time $\Delta t/2$ ahead of the corresponding values of η.

In order to initiate a wave field in the model, the values of Qx and Qy(at time $t = 0$) and of η(at time $t = -\Delta t/2$) are chosen, in the examples given here, to represent sinusoidal waves propagating over the whole model area. The waves are moving in a negative x direction and have initial height $2A_{i,j}$, and wave directions $\theta_{i,j}$ calculated from linear wave theory for refraction and shoaling on a plane beach. All shadow zones, behind breakwaters, etc., have the initial condition $Qx^0 = Qy^0 = \eta^{-\Delta t/2} = 0$.

Boundary values are required for the Qx and Qy. The upwave conditions form the driving boundaries and so generate the wave field in the model during the integration period. The downwave boundaries and internal boundaries (breakwater, etc.) are calculated in such a way that any reflectivity from zero to unity can be specified(Tanimoto et al., 1975). The driving boundaries require some refinement in order that reflected waves travelling back towards the offshore boundary pass out the model and are not re-reflected. This has been achieved by comparing the calculated values of Qx in the grid row adjacent to the driving boundary with the required driving values. The downwave boundary values of Qx and Qy are calculated from the histories of Qx and Qy on the adjacent upwave grid row. A weighting factor AF and a time delay τ are calculated for a given reflectivity r in such a way that the boundary value may be expressed as: (Copeland, 1985)

$$Q^{t}_{xn,j,j} = AF\ Q^{t-\tau}_{xn-1,j} \tag{16}$$

where

$$AF = \frac{1 - r}{[\ (1+r)^2 \sin^2(k\Delta x \cos\theta) + (1-r)^2 \cos^2(k\Delta x \cos\theta)\ ]^{1/2}} \tag{17}$$

and

$$\tan(\omega\tau) = \frac{1+r}{1-r} \tan(k\Delta x \cos\theta) \tag{18}$$

For a wave propagating in a discontinuous medium(e. g. a finite-difference mesh) the phase speed is changed from the expected $C(=\omega/k)$ to a value which satisfies the finite-difference form of the wave equations. Note that the numerical stability requires C. F. L. stability condition. Wave heights are calculated at the each grid location after each wave period has elapsed from the root-mean-square value of η. The value of wave angle θ, in the first instance, be obtained from Snell's Law. However, after one or more wave periods of integration time have elapsed, values of θ can be obtained using values of Qx and Qy(Copeland, 1985).

4. Discussion

Fig. 3 shows that the numerical results of parbolic and hyperbolic models and experimental results of Ito and Tanimoto(1972) are indicated for the comparison. Since the Neumann boundary condition is used in a case of the parabolic model, computations are performed upto five times of wave length along the both sides of y direction from the center. In the case of hyperbolic model which uses the arbitary reflectivity boundary condition, computations are performed upto four times of wave length. Both numerical analyses show satisfactory agreement with experimental results. In the view of the physical meaning, the hyperbolic equation represents wave propagation phenomena more reasonably than the parabolic equation. So it was confirmed that the experimental model also agree better with the results of the hyperbolic model than those of the parabolic model as shown in Fig. 3.

Fig. 4 shows the location of detached breakwater, breakwater with a gap, and profile sections for analysis. Both results of this model using hyperbolic equation and Copeland's model on the detached breakwater - conditions are normal wave incidence and horizontal bottom - are compared in Fig. 5, and it shows that agreement is good. As shown in Fig. 6, standing waves appear in front of breakwater, and wave energy are propagating in the direction of wave crest line. The differences of wave hight ratio in the case of bottom slope $\leqq$ 0. 02 are very small as shown in this figure. It means that the effect of shoaling is smaller than diffraction. But the effect of reflection appears to be considerable in the case of bottom slope = 0. 04.

Fig. 7 is the plotting results applied to the vicinity of breakwater with a gap of one wave length and 60° of incident wave angle on the horizontal bottom, it shows a fair agreement with the material of Shore Protection Manual(1984) which was calculated by Johnson in 1952. He simplified the Penny and Price solution that water wave diffraction is analogous to the diffraction of light. A validity of the hyperbolic model is proved by this figure. Fig. 8 presents the results of numerical analysis which has conditions with incident angle 30° and 60° in the range of bottom slope 0 and 0. 02 , and shows the effects of

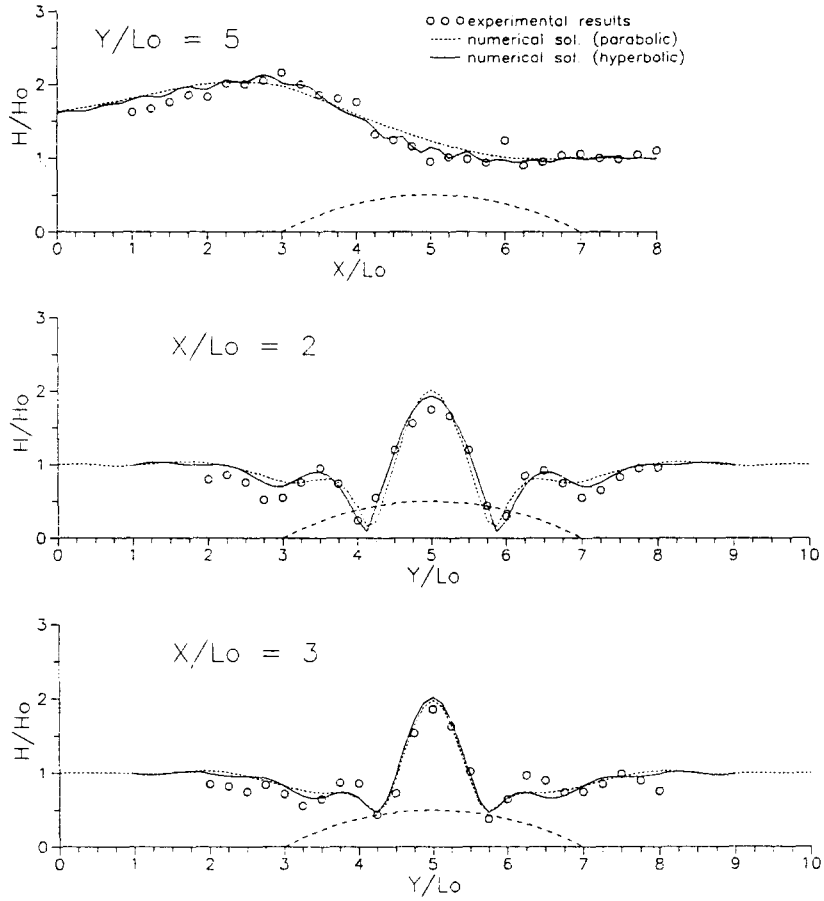

Fig. 3. Comparision of wave heights H/H_o for oiroular shoal between computational results and experimental results of I to and Tanimoto(1972).

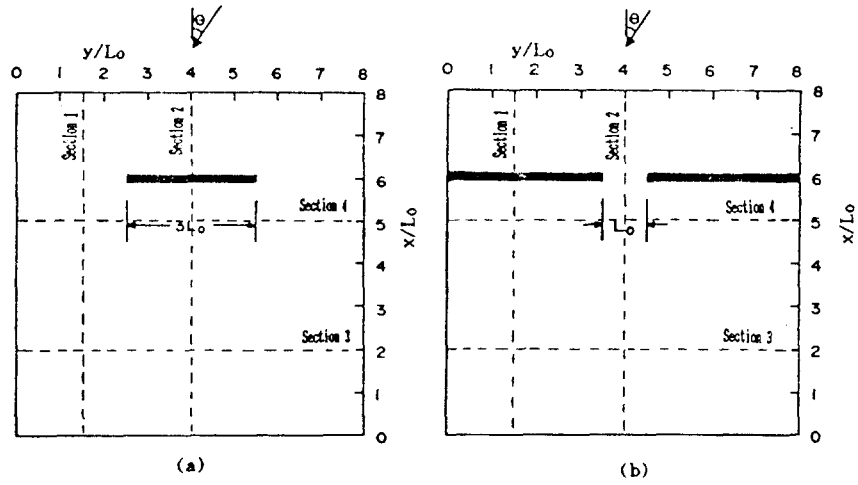

Fig. 4. Locations of breakwaters and sections in the analysis area; (a) detached breakwater, (b) breakwater with a gap.

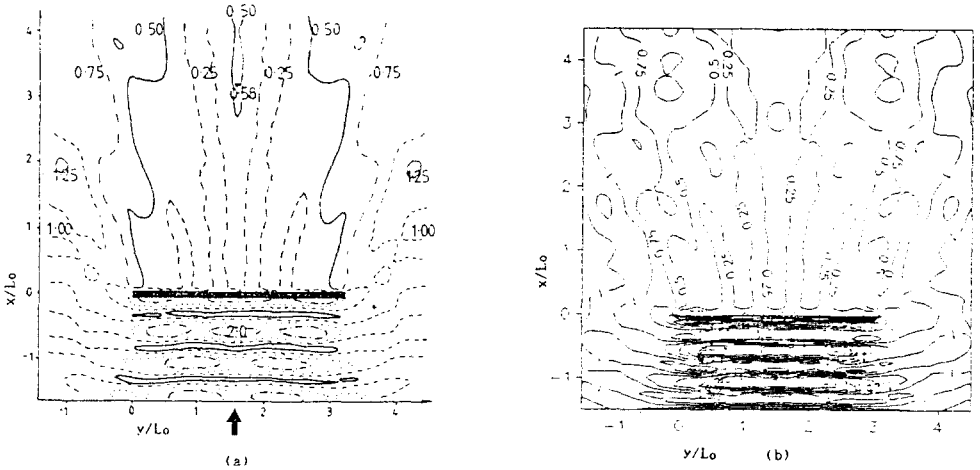

Fig. 5. Contours of wave lieights H/H_o on detached breakwater in the case of normal wave incidence and horizontal bottom; (a) results of Copeland's model, (b) results of this paper.

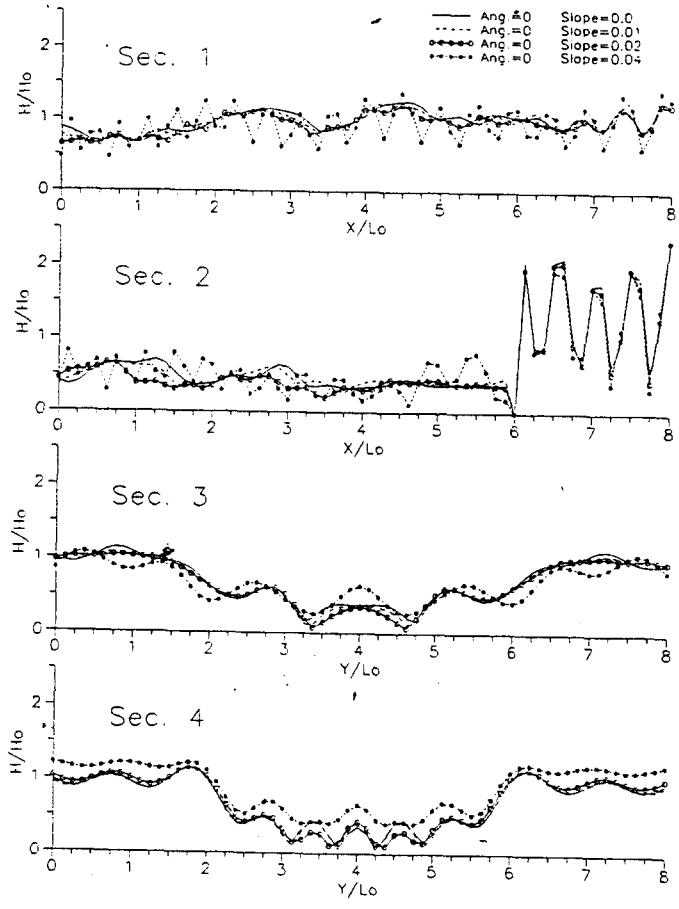

Fig. 6. Wave heights in each section for the detached breakwater; normal wave incidence and various bottom slope.

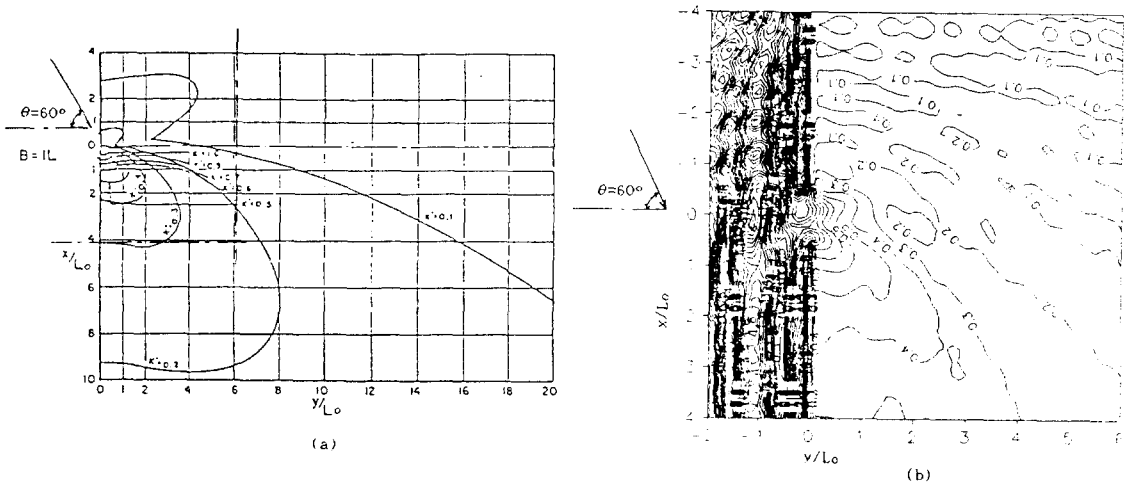

Fig. 7. Contours of wave heights H/H_0 for the breakwater with a gap in the case of incident wave angle 60° and horizontal bottom; (a) material of shore protection Manual, (b) results of this paper.

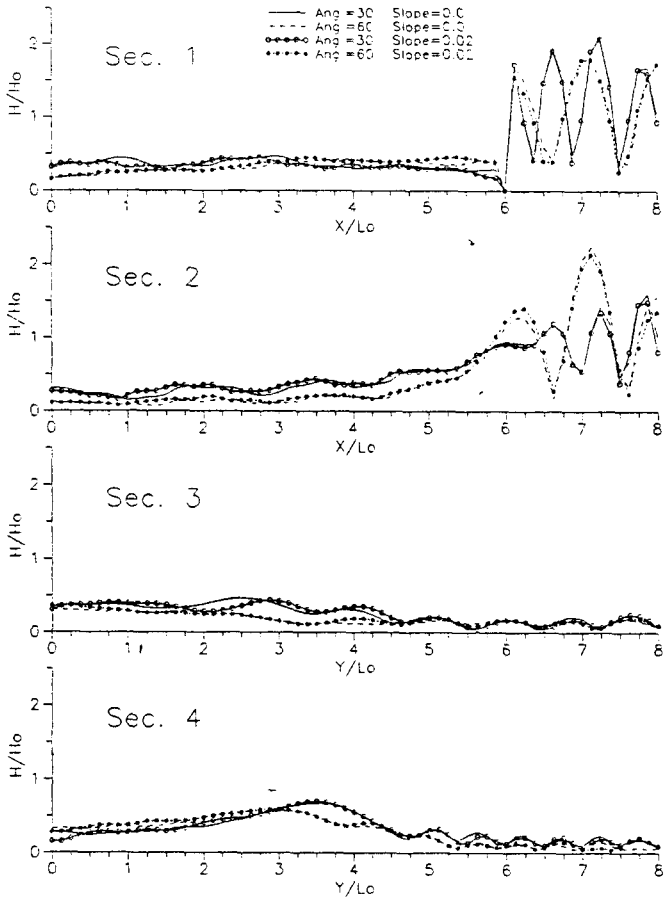

Fig. 8. Wave heights in each section for the breakwater with a gap; varying incident wave angle from 30° to 60° and bottom slope from 0.0 to 0.02

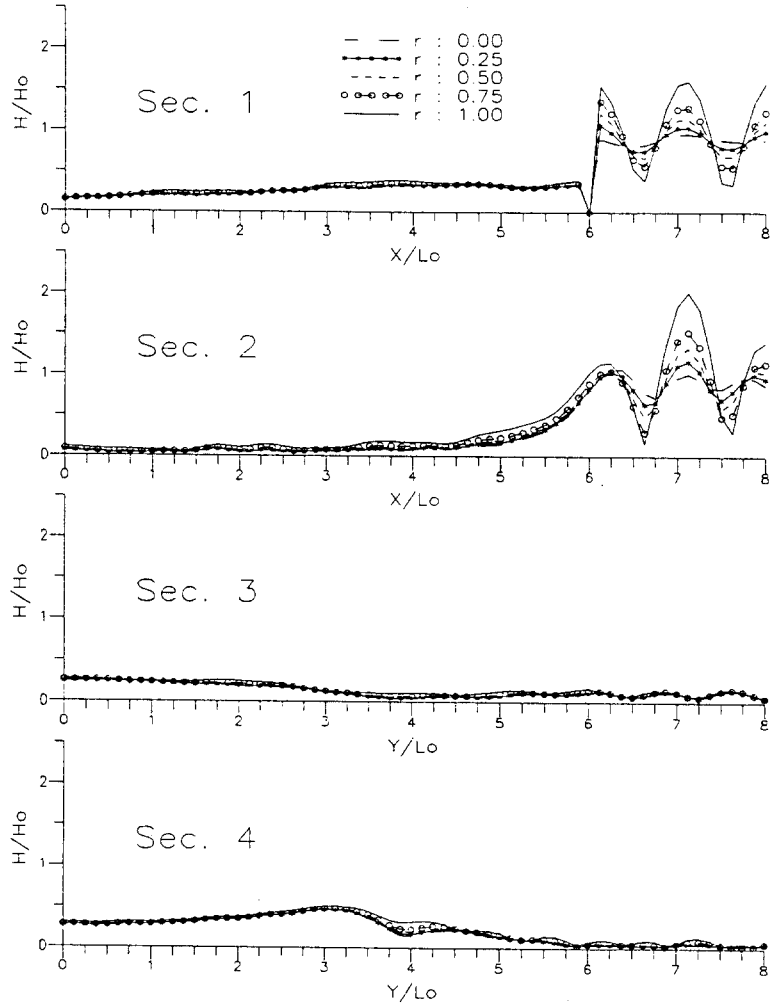

Fig. 9. Wave heights in each section for the breakwater with a gap; 60° of incident wave angle, horizontal bottom and various reflectivity of breakwater.

diffraction and reflection well. The effect of bottom slope on the wave height ratio did not appear significantly, it means that the effect of refraction is smaller than that of diffraction. It is also shown that the patterns of the standing wave in front of the breakwater are formed differently with incident angle. The reason that wave hight distributions of incident angle 60° are lower than of incident angle 30° is that the imaginary gap width is reduced by enlarging the incident angle.

Fig. 9 shows the results of numerical analysis which has conditions with the various reflectivity of 0 to 1.0, the incident angle 60° and the constant water depth. The variation of wave amplitude in front of breakwater are large, depending on the reflectivity. But effect of the reflecivity is very small at the backside of breakwater.

5. Conclusion

The numerical models of parabolic equation and hyperbolic equations were developed, and performed on the area of the submerged circular shoal. The results of the numerical models were compared with the experimental results. Moreover, the hyperbolic model was performed in the vicinity of breakwater where reflections are expected, and the results of this model were compared with existing materials. In many cases where the bottom slope, the incident angle and the reflectivity were different, the hyperbolic model was performed to show the applicability on the property study of wave transformation. From the numerical analysis, following conclusions are drawn:

1) Both results of the parabolic and the hyperbolic models, performed on the shoal, agreed well with the experiment of Ito and Tanimoto, and the hyperbolic model was superior than the parabolic model on accuracy.

2) The results of the hyperbolic model, carried out in the vicinity of breakwater, accorded well with the existing materials such as Copeland' model(1985) and Shore Protection Manual.

3) The effect of diffraction was stronger than that of refraction on the small bottom slope, the patterns of the standing wave in front of the breakwater were varied with incident angle, and the wave heights were enlarging in proportion to reflectivity at the front of breakwater.

References

1. Berkhoff, J. C. W., 1972. Computations of Combined Refraction-Diffraction, Proc. 13th Conf. Coastal Eng. ASCE, Chap. 26.
2. Booij, N., 1981. Gravity Waves on Water with Non-uniform Depth and Current. Delft University of Tech., Dep. Civil Eng., Report No. 81-1.
3. Copeland, G. J. M., 1985. A Practical Alternative to the "Mild-Slope" Wave Equation, Coastal Engineering, pp. 125-149.
4. Ito, Y. and Tanimoto, K., 1972. A Method of Numerical Analysis of Wave Propagation-Application of Wave Refraction and Diffraction, Proc. 13th Conf. Coastal Eng., ASCE, Chap. 26.
5. Kirby, J. T., 1983. A Parabolic Equation for the Combined Refraction-Diffraction of Stokes Waves by Mildly Varying Topography, J. Fluid Mech., Vol. 136, pp. 453-466.
6. Lee, C. H., 1990. Numerical Analysis of Water-Wave Transformation with Refleced Waves, MS Thesis, Department of Civil Engineering, Hanyang University. (in Korean)

7. Lee, J. K. and Lee, J. I., 1990. Numerical Analysis of Nonlinear Effect of Wave on Refraction and Diffraction, Journal of Korean Society of Coastal and Ocean Engineers, Vol. 2, No. 1, pp. 51-57. (in Korean)
8. Liu, P. L-F., 1983. Wave-Current Interaction on a Slowly Varying Topography , J. Geophys. Res., 88, pp. 4421-4426.
9. Liu, P. L-F. and Tsay, T-K., 1984. Refraction-Diffraction Model for Weakly Nonlinear Water Waves, J. Fluid Mech., Vol. 141, pp. 265-274.
10. Radder, A. C., 1979. On the Parabolic Equation Method for Water Wave Propagation, J. Fluid Mech., 95, pp. 159-176.
11. Tanimoto, K., Kobune, K., Komatsu, K., 1975. Numerical Analysis of Wave Propagation in Harbours of Arbitrary Shape, Rep. Port Harbour Res. inst., Jpn., 14(3).
12. U. S. Army Coastal Engineering Research Center, 1984. Shore Protection Manual.
13. Yoo, D. H., O'Connor, B. A. and McDowell, D. M., 1988. Mathematical Models of Wave Climate for Port Design, Proc Instn Civ. Engrs, part 1, pp. 513-530.